

Thermal dark photon and a long-lived axion mediator

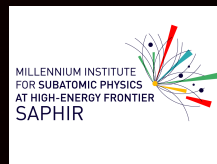
Bastián Díaz Sáez, PUC-SAPHIR

Sorbonne Université, Campus Pierre-et-Marie-Curie, Paris,
France

28 de junio de 2024

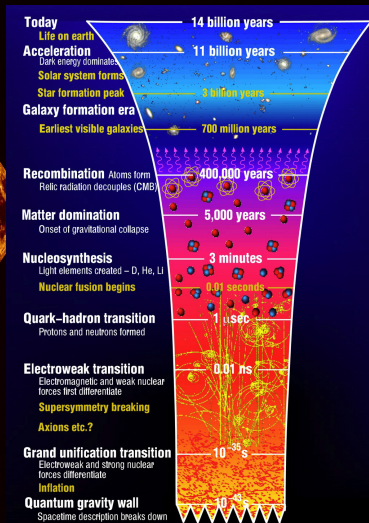
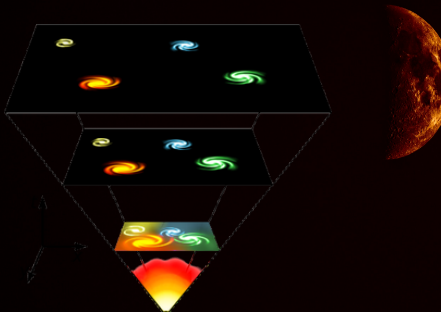


PONTIFICIA
UNIVERSIDAD
CATÓLICA
DE CHILE



Our history

An expanding thermal universe!

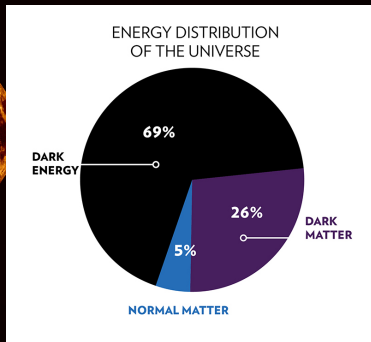


Energy in the universe

Dark matter (DM) evidence:

- Large-scale structure of the universe.
- Cosmic microwave background.
- Rotational curves.

$$\Omega_{\text{DM}} h^2 \equiv \frac{\rho_{\text{DM}}}{\rho_c} = 0.12$$



DM candidates

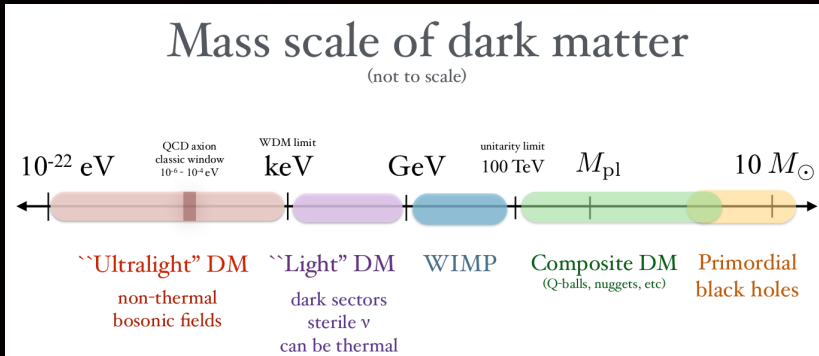


Figura 1: Some of the possibilities for the DM (TASI T. Lin 1904.07915).

DM production mechanisms

There are many ways to produce DM:

- Thermal: freeze-out.
- Non-thermal: misalignment, freeze-in, DW mechanism, gravitational production...

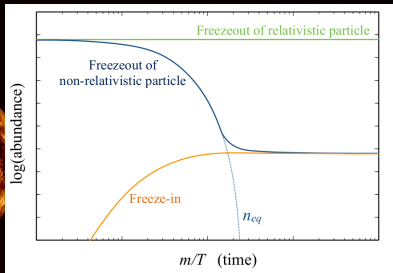


Figura 2: Different mechanisms of DM production (TASI T. Lin 1904.07915).

DM production mechanisms

There are many ways to produce DM:

- Thermal: **freeze-out**.
- Non-thermal: misalignment, freeze-in, DW mechanism, gravitational production...

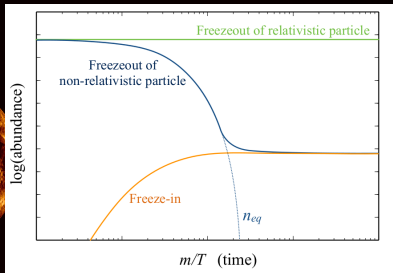


Figura 3: Different mechanisms of DM production (TASI T. Lin 1904.07915).

Leptophilic dark matter

- Let us consider a Majorana fermion χ coupled to the SM leptons via a scalar mediator ϕ (Honorez et al 2019, JCAP).

$$\mathcal{L} \supset -m_\chi \bar{\chi}\chi - (\lambda_\chi \phi \bar{\chi} l_R + h.c.) - \frac{1}{2} m_\phi^2 |\phi|^2 - \lambda_H |H|^2 |\phi|^2$$

- New parameters: $(m_\chi, m_\phi, \lambda_\chi, \lambda_H)$.

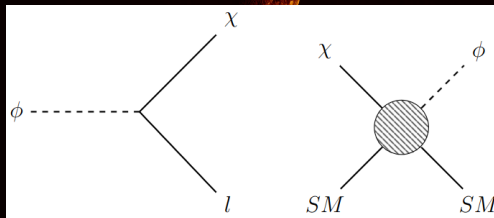


Figura 4: Some Feynman diagrams for relevant process in the calculation of the relic abundance.

DM production mechanisms

- If $m_\chi < m_\phi$, χ is the DM candidate.
- Solve the Boltzmann(s) equation(s) for χ and ϕ .

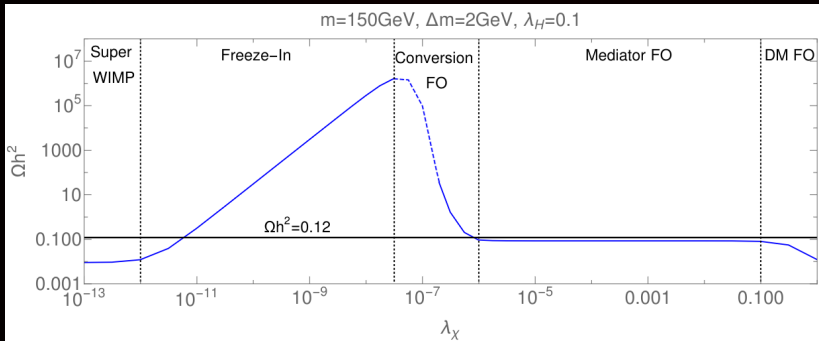


Figure 5: DM abundance as a function of the Yukawa coupling for $m_\chi = 150$ GeV, $\Delta m = 2$ GeV and $\lambda_H = 0.1$.

Outline

- 1 Model.
- 2 Relic.
- 3 Long-lived particles.
- 4 Conclusions



Lagrangian

Let us add a $U(1)$ gauge symmetry to the SM plus a singlet pseudo-scalar. Assuming a dark-CP symmetry $(A', \phi) \rightarrow -(A', \phi)$, the Lagrangian is:

$$\mathcal{L} \supset -\frac{1}{4}F'_{\mu\nu}F'^{\mu\nu} - \frac{1}{2}m_{\gamma'}^2 A_\mu'^2 + \frac{1}{2}(\partial_\mu\phi)^2 - \frac{1}{2}m_\phi^2\phi^2 - \lambda_{HS}\phi^2|H|^2$$

with $F'_{\mu\nu}$ the $U(1)$ dark photon field strength, and H the Higgs doublet.

No vev for ϕ .

Due to the darkCP, **no kinetic mixing between A_μ and A'_μ .**

Lagrangian

- ① A five-dimensional operator is allowed (Kaneta et al 2016, PLR):

$$\mathcal{L}_5 = \frac{g_D}{4} \phi F'_{\mu\nu} \tilde{F}^{\mu\nu},$$

where the dual field strength defined as

$$\tilde{F}^{\mu\nu} = \frac{1}{2} \epsilon^{\mu\nu\alpha\beta} F_{\alpha\beta}.$$

- ② If $m_{\gamma'} < m_\phi$, γ' is a DM candidate and ϕ an unstable mediator.

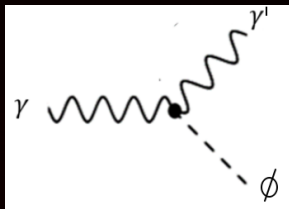


Figura 6: Vertex.

Four free parameters:

$$m_{\gamma'}, m_\phi, g_D, \lambda_{HS}$$

Previous and present studies

Various studies of this scenario have been carried out. Some of them:

- 1 Freeze-in (Kaneta et al 2017).
- 2 Supernova constraints (A. Hook et al, 2021 JHEP).
- 3 CMB (A. Hook et al, 2023 JHEP).
- 4 Thermal dark axion portal, (H. Hong et al 2024 JHEP)
- 5 Freeze-in history (Arias P., B.D.S, Jaeckel J., Arza A., under construction!).

Thermal dark photon DM

- ① Mass focus $\text{GeV} \lesssim (m_{\gamma'}, m_\phi) \lesssim \text{TeV}$, with $m_{\gamma'} < m_\phi$.
- ② $T \gtrsim (m_{\gamma'}, m_\phi)$: dark and visible sectors in thermal equilibrium.
- ③ Chemical equilibrium (CE) **within the dark sector**

$$\Gamma(\gamma' + 0 \leftrightarrow \phi + 0) \gg H \quad (1)$$

at the epoch of freeze-out of the DM is not necessarily guaranteed in the whole parameter space (Garny et al PRD 2027, D'Agnolo et al 2017 PRL).

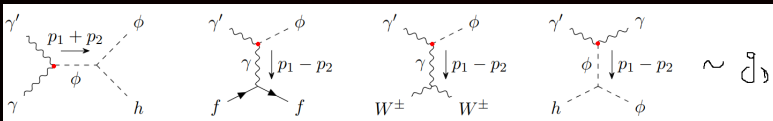


Figura 7: Feynman diagrams relevant for $\Gamma_{\gamma' \rightarrow \phi}$ conversions.

Full Boltzmann equations

The cBE for the yields is given by

$$\frac{dY_{\gamma'}}{dx} = \frac{1}{3H} \frac{ds}{dx} \left[\langle \sigma_{\gamma'\gamma'00v} \rangle (Y_{\gamma'}^2 - Y_{\gamma',e}^2) + \langle \sigma_{\gamma'\phi 00v} \rangle (Y_{\gamma'} Y_{\phi} - Y_{\gamma',e} Y_{\phi,e}) \right. \\ \left. + \frac{\Gamma_{\gamma' \rightarrow \phi}}{s} \left(Y_{\gamma'} - Y_{\phi} \frac{Y_{\gamma',e}}{Y_{\phi,e}} \right) + \frac{\Gamma_{\phi}}{s} \left(Y_{\phi} - Y_{\gamma'} \frac{Y_{\phi,e}}{Y_{\gamma',e}} \right) \right]$$

$$\frac{dY_{\phi}}{dx} = \frac{1}{3H} \frac{ds}{dx} \left[\langle \sigma_{\phi\phi 00v} \rangle (Y_{\phi}^2 - Y_{\phi,e}^2) + \langle \sigma_{\gamma'\phi 00v} \rangle (Y_{\gamma'} Y_{\phi} - Y_{\gamma',e} Y_{\phi,e}) \right. \\ \left. - \frac{\Gamma_{\gamma' \rightarrow \phi}}{s} \left(Y_{\gamma'} - Y_{\phi} \frac{Y_{\gamma',e}}{Y_{\phi,e}} \right) - \frac{\Gamma_{\phi}}{s} \left(Y_{\phi} - Y_{\gamma'} \frac{Y_{\phi,e}}{Y_{\gamma',e}} \right) \right]$$

with 0 indicating a SM state, and $Y_{\gamma',e}$ and $Y_{\phi,e}$ the equilibrium yields. The rate of particle conversions per DM particle is given by

$$\Gamma_{\gamma' \rightarrow \phi} = \sum_{k,l} \langle \sigma_{\gamma' k \rightarrow \phi l v} \rangle n_{k,e}, \quad (2)$$

with k, l a SM state. Here $n_{k,e} \propto T^3$.

Full Boltzmann equations

Implementation: LanHEP \rightarrow micrOMEGAs 5.3.41. The latter solves the cBE using two different solvers

- 1 darkOmega : It assumes **chemical equilibrium (CE) within the dark sector for all T** . This is:

$$\frac{dY_{DM}}{dx} = \frac{s\langle\sigma v_{\text{eff}}\rangle}{Hx} (Y_{DM}^2 - Y_{DM,eq}^2)$$

$$\langle\sigma v_{\text{eff}}\rangle \simeq \frac{1}{g_{\text{eff}}^2} \sum_{ij} r_i r_j \langle\sigma v\rangle_{ij} \quad \text{with} \quad g_{\text{eff}} = \sum_i r_i$$

$$\text{and} \quad r_i = g_i (1 + \Delta_i)^{3/2} \exp(-x_f \Delta_i).$$

where it was assumed that $Y_{\gamma'}/Y_{\gamma'e} = Y_{\phi}/Y_{\phi e}$.

- 2 darkOmegaN : No CE assumption, then it solves the full cBE.

LanHEP software package

MicrOMEGAs: a code for the calculation of Dark Matter Properties including the relic density, direct and indirect rates in a general supersymmetric model and other models of New Physics

Results: relic abundance

Expected behavior relic abundance with a similar pattern as in the leptophilic scenario.

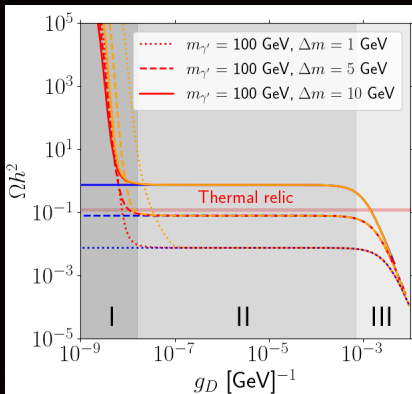


Figura 8: Relic abundance as a function of g_D . The red curves are obtained with `darkOmegaN`, the blue ones with `darkOmega`, and the orange ones without considering conversion processes. The regions shown as I, II and III, correspond to the case $\Delta m = 5$ GeV. Besides, $\lambda_{HS} = 1$.

Yield and rates of region I (coscattering)

- ① In the coscattering regime the DM decouples earlier.
- ② Conversion rates comparable to H rate.

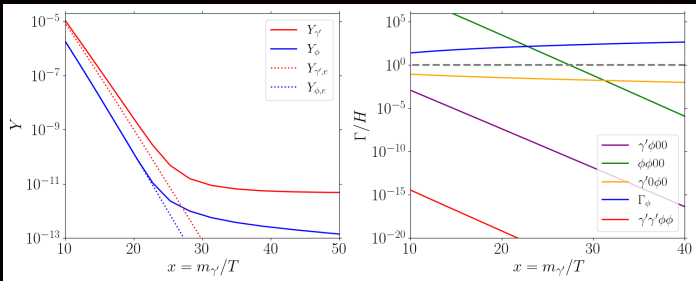


Figure 9: (left) Yield evolution for the DP and the ALP as a function of the inverse of the temperature. Here we consider $m_{\gamma'} = 100$ GeV, $\Delta m = 5$ GeV, $g_D = 10^{-8}$ GeV $^{-1}$ and $\lambda_{HS} = 1$. (right) Particle interactions rates over Hubble rate as a function of the inverse temperature. "0" here refers to a SM particle.

Long-lived particles (LLP)

- 1 In collider environments: particles that decay far from the interaction vertex ("long" lifetimes).
- 2 In the SM we have some LLP.
- 3 Different experiments to search for new LLP: ATLAS, CMS, FASER, MATUSHLA, etc...

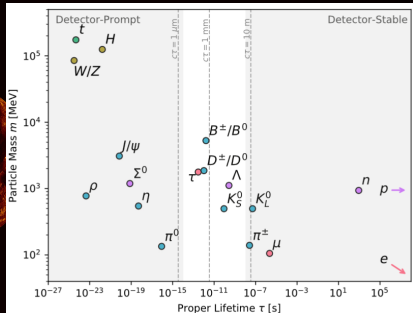


Figura 10: Lifetime of some SM particles.

Long-lived particles (LLP)

At the LHC, we may pair produce ALPs as **displaced vertex** from

$$p + p \rightarrow \phi + \phi, \quad \phi \rightarrow \gamma' + \gamma$$

① $\sigma(p + p \rightarrow \phi + \phi) \propto \lambda_{HS}^2$.

② $\Gamma(\phi \rightarrow \gamma' + \gamma) \propto g_D^2$, then $c\tau = \frac{1}{g_D^2}$. ($\text{Br}_{\phi \rightarrow \gamma' \gamma} = 1$).

Remember that the thermal dark-axion scenario gives the correct relic abundance for EW masses of the new states and for $\lambda_{HS} = 1$ and $g_D \ll 1$!

Prospects of LLP at detectors

- ① Small g_D : region I and II (coscattering and mediator FO, respectively).
- ② Displacement vertex in the distance reach of LHC and MATHUSLA.

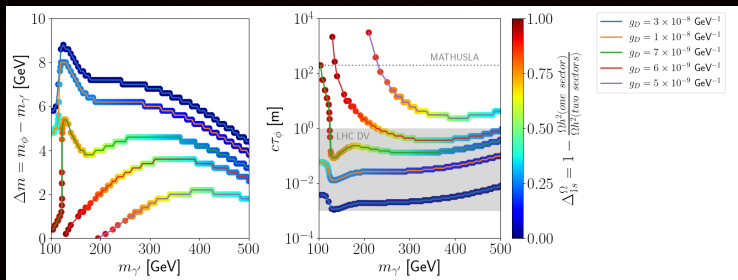


Figure 11: Points fulfilling the correct relic abundance. The color of each point represents $\Delta\Omega_{1s}^\Omega$. Here we have set $\lambda_{HS} = 1$. In the plot in the right, we highlight the expected distance of MATHUSLA from the proton-proton colliding point, and the region expected for displace vertex (DV) in the detectors at the LHC.

Conclusions

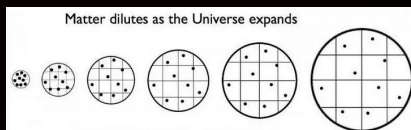
- 1 Several DM candidates and production regimes: freeze-in, freeze-out (**coscattering**, **mediator FO**, (co)annihilations), misalignment mechanism, etc...
- 2 We have studied a dark axion portal scenario. For very small g_D , we enter into the mediator FO and coscattering regime: **relic abundance successfully obtained**.
- 3 Long-lived particles are a natural consequence of the **coscattering regime**, and also in the mediator FO regimes. ALPs can be (eventually) seen at the different experiments!
- 4 Future: A more precise analysis of the viability of the model at the LHC and future experiments (e.g. Matushla).

Appendix



(Early universe) Expansion vs interactions

H versus Γ



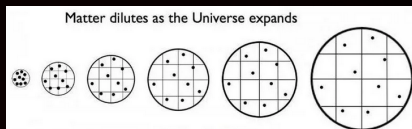
- The interacting particles are **in** an expanding universe.
- The expansion of the universe $H \approx T^2/M_P$, M_P Planck mass.
- Neutrinos: $\sigma_w \sim G_F^2 T^2$, $G_F \sim 10^{-5} \text{ GeV}^{-2}$ (At $T \sim 1 \text{ MeV}$, $\sigma_w \sim 10^{-16} \text{ GeV}^{-2}$).

$$\frac{\Gamma}{H} \sim \left(\frac{T}{1\text{MeV}} \right)^3$$

- Thomson scattering, $e^- + \gamma \rightarrow e^- + \gamma$, $\sigma = 1 \text{ bn} \approx 10^3 \text{ GeV}^{-2}$.

(Early universe) Expansion vs interactions

H versus Γ



- **What about a WIMP?**
- Assume that S initially was in TE with the SM:
 $n_S(t_0) = n_{S,eq}(t_0)$.
- The expansion can deviate S from its TE at some T : Lost of CE.
- We want to know n_S . Solve Boltzmann equation (BE):

$$E(\partial_t - H\mathbf{p} \cdot \nabla_{\mathbf{p}})f_S = C[f_S]$$

(Early universe) The freeze-out of a WIMP

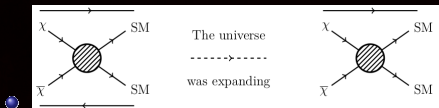


Figure 12: At high T the rates of the forward and reverse reactions occurs at an equal rate. At $T \lesssim m_\chi$, the equilibrium is broken.

- The **Boltzmann equation** (BE) $\hat{L}[f_\chi] = C[f_\chi]$ to track the abundance of χ in a FRW universe:

$$E(\partial_t - H\mathbf{p} \cdot \nabla_{\mathbf{p}})f_\chi = C[f_\chi] = C_{el}[f_\chi] + C_{ine}[f_\chi]$$

- The picture of DM chemically decoupling (but in kinetic equilibrium) is described as a dilute ideal non-relativistic gas fulfilling

$$f_\chi(t, \mathbf{p}) \approx A(T)f_{\chi,eq}(t, \mathbf{p}) = e^{\beta\mu(T)}e^{-E/T} \quad (3)$$

with $\beta = 1/T$.

(Early universe) The freeze-out of a WIMP

- One can recast the BE for $n_S \equiv N_S/a^3$:

$$\dot{n}_S + 3Hn_S = -\langle\sigma v\rangle(n_S^2 - n_{S,eq}^2)$$

- To get rid of H in the equation, change of variables:

$$Y_S = n_S/s, \quad x \equiv m_S/T$$

with $s = 2\pi^2/45g_{*s}(T)T^3$ (entropy density), then

$$\frac{dY_S}{dx} = -\frac{\lambda}{x^2} [Y_S^2 - Y_{S,eq}^2], \quad x \equiv m_S/T$$

where $\lambda \sim \langle\sigma v\rangle$ and $Y_{eq}(x) \sim e^{-x}$.

(Early universe) The freeze-out of a WIMP

Simplest scenario: A real gauge singlet scalar S .

$$\mathcal{L} \supset m_S^2 S^2 + \lambda_{SH} S^2 |H|^2 \quad (4)$$

For $m_S = 100$ GeV, the relic depends only on λ_{SH} .

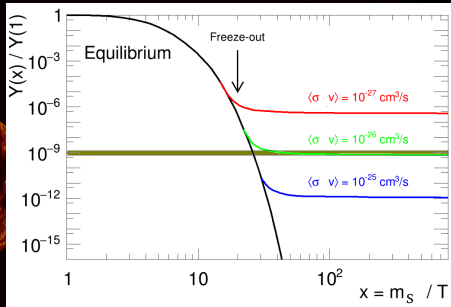
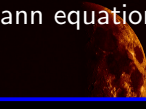


Figure 13: DM particle abundance showing chemical decoupling.

$$\Omega h^2 \propto Y_S^\infty m_S \approx 0.12$$

Chemical equilibrium assumption

- 1 In the first case, $\Gamma_{1 \rightarrow 2} \gg H$, CE at freeze-out.
- 2 Two coupled Boltzmann equations (cBE) can be reduced to a single one:


$$\dot{n} + 3Hn = -\langle \sigma_{eff} v \rangle (n^2 - n_{eq}^2)$$

where $n \equiv n_1 + n_2$, and $\langle \sigma_{eff} v \rangle$ is the effective cross section.

Relic abundance as a function of g_D

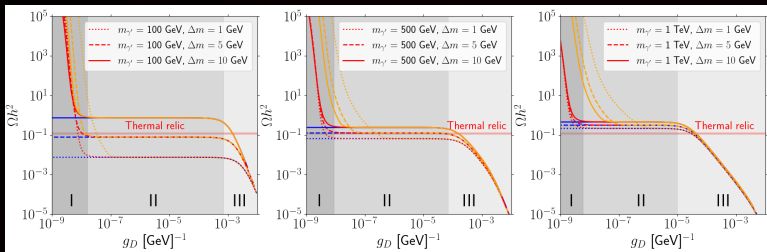


Figura 14: Relic abundance. The red curves are obtained with darkOmegaN, the blue ones with darkOmega, and the orange ones without considering the process 1020. The regions shown in each plot as I, II and III, correspond to the case of $\Delta = 5$ GeV. In all the plots we have set $\lambda_{HS} = 1$.

Results: $\Delta m \gtrsim 1 \text{ GeV}$

- 1 Viable DM masses from $\sim 50 \text{ GeV}$.

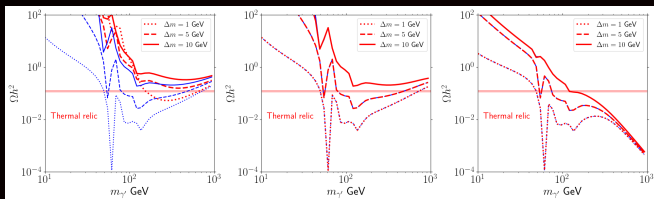


Figure 15: (top) Relic abundance as a function of $m_{\gamma'}$. In the left, middle and right columns we consider $g_D = 6 \times 10^{-9} \text{ GeV}^{-1}$, 10^{-5} GeV^{-1} and 10^{-3} GeV^{-1} , respectively. The red and blue lines are obtained with `darkOmegaN` and `darkOmega`, respectively. Here we set $\lambda_{HS} = 1$. (bottom) Relic abundance as a function of λ_{HS} , for $m_{\gamma'} = 500 \text{ GeV}$. The values of g_D follows the same order than the top row of plots.

Results: $\Delta m \leq 1$ GeV

- 1 Viable DM masses from ~ 30 GeV.

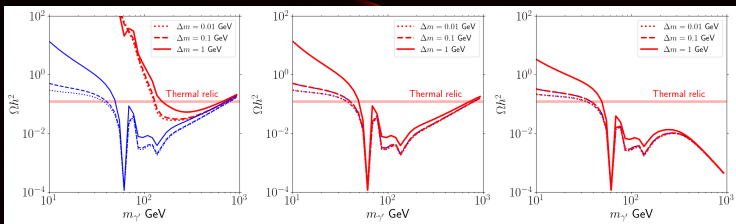


Figura 16: Same than before but in the small mass shift scenario.